Behaviour of Connections for Hybrid FRP/Steel Shear Walls

M. Dakhel [1*], T. Donchev [2*] and H. Hadavinia [3]
[1 *]Department of Civil Engineering, Kingston University, UK.
Email: dakhel.m@hotmail.com
[2 *]Department of Civil Engineering, Kingston University, UK.
Email: T.Donchev@kingston.ac.uk
[3] Department of Mechanical Engineering, Kingston University, UK.
Email: H.Hadavinia@kingston.ac.uk

Abstract
The design of more efficient and lightweight steel shear walls (SSW) has led to research in incorporation of fibre reinforced polymer (FRP) composite in the infill plate of shear wall systems. As a result, understanding the behaviour of the connections between the hybrid steel/FRP infill plate and the fish plate of the surrounding frame elements has become necessary. In this paper, energy absorption and load carrying capacity of FRP-to-steel connections has been investigated to develop a more efficient hybrid steel/FRP shear wall system. Monotonic displacement controlled loading of bolted connections, representing the connections in steel and hybrid shear walls, were conducted to complete failure. The specimens had dimensions of 125 mm × 70 mm with varying factors some of which were using two and three bolts connections, applying additional GFRP strips, using adhesive between the steel plate and the internal layer of GFRP as well as applying adhesive between the clamping plate and the FRP around the bolted area. A detailed comparison between the specimens in aspects of energy absorption, load capacity and modes of failure is provided.

Keywords: Shear walls; GFRP; Load capacity; Energy absorption; Failure modes

1. Introduction

Steel shear wall (SSW) systems are one of the fast-developing lateral resisting systems utilised in medium to high-rise buildings. These systems have high ultimate capacity, well defined plastic behaviour and high energy absorption capacity. They also have higher stiffness, lighter weight, reduced construction times and costs in comparison with reinforced concrete shear walls (Yadollahi et al., 2015). However, SSW's require accurate and sometimes complex fixings to the boundary frame elements using either bolts or welds (Gardner, 2015)(Seilie and Hooper, 2005). In addition, SSWs could appear more expensive for specific types of buildings and require a higher level of quality control in comparison with reinforced concrete shear walls. Thin plate shear walls dissipate energy by plastic deformations through the tension field action that develops in the infill plate during the non-linear post buckling phase. The tension field action is formed at lower loads for thinner plates than for thicker or stiffened steel plates. Recent research adopts thin unstiffened steel plate shear walls (SPSW) where tension field action is utilised to resist lateral forces(Bahrebar et al., 2016; Shekastehband et al., 2017; Tsai et al., 2010). However, the boundary elements are utilised for capacity design to remain elastic and provide sufficient strength to help develop the tension fields (Bhowmick et al., 2014). The 337

m tall tower in Tianjin, China is one of the very first practical examples of thin steel plate shear walls. The use of the thin plate shear wall system was favoured over a concrete system due to the size of the concrete systems that will impact rentable space leading to financial impacts. Steel systems with perimeter moment frames and braced cores were also eliminated due to requiring 20-25% more steel to satisfy the same structural capacity (Sarkisian et al., 2011). Seismic design guides such as the Chinese JGJ 99 – 98, American seismic provisions for structural steel buildings and building standard law of Japan give provisions for the sizing and design of SSW (American Institute of Steel Construction, 2016; Architecture & Building Press, 1998; Gardner, 2015; Japan. Kensetsushåo. Jåutakukyoku. Kenchiku Shidåoka. and Nihon Kenchiku Sentåa., 2004; Sabelli and Bruneau, 2006).
More recently a new generation of hybrid shear walls using steel/fibre reinforced polymer (FRP) composite has been under development. In the new design, FRPs are used in conjunction with steel infill plate in a SSW system to further increase the strength and the energy absorption capacity of the system. The use of FRP will help reduce the individual member weight via replacing some of the steel section with FRP material, which is up to 70% lighter than steel. It will also contribute to a more overall lighter structure and hence a more cost effective structural design especially for high-rise buildings. Life cycle costing of FRP material in the construction industry indicates that the application of FRP material offers a viable economical solution when considering external costs such as gains in sustainability (Ilg et al., 2016). At the same time FRP layers will be extremely beneficial in preventing the potential corrosion of the steel infill plate with much higher durability than any type of paint. However, the application process of FRP to steel requires high level of quality control for surface preparation and FRP finishing to ensure the best bond between the material and the steel plate.

Introducing FRPs in hybrid SSWs (HSSWs) presents complexities in the overall behaviour of the lateral resisting system and also creates more complex local behaviours around the connection of the infill plate and the boundary frame. These connections are vital for the development of stable and uniform tension field and also contribute to the overall energy dissipation of the SSW system.

According to Nateghi-Alahi and Khazaei-Poul (Nateghi-Alahi and Khazaei-Poul, 2012), if the principal fibre orientation is in the direction of the tension field this will enhance the shear strength, initial and secant stiffness as well as the cumulative energy dissipation. An experimental evaluation of the effects of different connections for SSWs, such as bolted and welded ones, was carried out by Choi and Park (Choi and Park, 2008). One of the relevant type of SSW infill plate connections was a steel infill plate welded to a 50 mm wide and 6 mm thick fish plate. The other was a bolted infill plate SSW system with a 100 mm × 6 mm primary fish plate and an 80 mm × 6 mm secondary fish with M20 at 100 mm spacing. The authors looked at the energy absorption and found that the two systems exhibited similar energy dissipation characteristics up to a drift ratio of 3.6% at which the bolted system reached its maximum displacement of 120 mm. The bolted SSW systems energy dissipation capacity was half that of the welded stem which can be attributed to the tearing of the plate at a displacement of 90 mm.

The connection of FRP joints can be classified into two main categories: (i) mechanically fastened joints and (ii) adhesively bonded joints. Net section tension, shear out, bearing, cleavage and slip modes of failure can be observed for mechanically fastened FRP in plane loaded joints. FRP connections that are bonded with adhesive are subjected to simultaneous multiple stresses such as shear, pealing, out of plane and in plane tension and compression stresses. Some of the main failure modes of adhesively bolted FRP joints are adhesive failure along the interface, cohesive failure along the adhesive bond line, fibre tear failure and stock break failure(Turvey, 2000; Zhou and Zhao, 2013). Rosner and Rizkalla (Rosner and Rizkalla, 1995) developed an analytical model and design recommendations for FRP bolted structural connections. Specimens were tested and failure envelopes for fibre orientations of 0°, 45° and 90° were developed with factors including the ratios of the diameter of the hole to width (d/w) and edge distance to hole diameter (e/d). Based on the developed envelopes, the efficiency and modes of failure such as net tension, cleavage and bearing could be estimated.

Hybrid GFPR/CFRP bolted double lap shear connections, with and without adhesive bonding, were assessed by Manalo et al., (Manalo et al., 2008). Crushing of fibres and bearing failure were observed for the bolted specimens without adhesive, while the bolted specimens bonded with adhesive exhibited bearing failure and eventually delamination between the GFRP and CFRP layers. The occurrence of delamination could be due to the sudden slip in adhesive that resulted in a release of high energy. They also evaluated the effects of level of applied torque of the bolts on the load capacity of the specimens and found that there is a slight increase in ultimate load capacity when the torque is increased.
Hai and Mutsuyoshi, (Hai and Mutsuyoshi, 2012) investigated Hybrid FRP (HFRP) double lap joints with steel plates bonded and bolted to pultruded HFRP laminates. The authors tested more than 42 specimens and analysed the ultimate load capacity and the failure modes. Their results showed that bolt located at the end distance of 4 times the hole diameter was the more robust design as it would develop a bearing mode of failure. The authors also assessed the effects of torque on the bolted and bonded specimens and stated that a high level of torque would reduce the adhesive thickness and result in slightly lower stiffness. The reduced thickness in the adhesive layer would result in lower bond strength and result in a higher likelihood of early slip between the plates.

Hybrid steel/FRP double lap connections with two bolts has been investigated by Petkune et al., and Dakhel et al., (Dakhel et al., 2016; Petkune et al., 2014) with the aim to assess the energy absorption, load capacity and failure mode characteristics for HSSW connection systems. Varying factors such as application of adhesive and additional layer for FRP around the bolted areas to improve the above mentioned characteristics of the connections were investigated. It was found that there is an increase in load carrying capacity and energy absorption for specimens by applying adhesive between the two clamping plates of the double lap joint. Dakhel et al., further investigated the effects of applying additional FRP strips around the bolted zone of the double lap connection. It was found that there is an increase in both the energy dissipation and load carrying capacity of the tested connections.
Extensive experimental research was conducted on double-lap hybrid FRP–steel bolted connections assessing parameters such as number of washers, clamping torque, diameter of

hole, and spacing of bolts, where it was recommended that two washers be used with snug-tight knots in standard sized holes (Abou El-Hamd et al., 2018).In another publication parameters such as sheared edge distance and rolled edge distance and spacing between bolts on FRP-steel anchored connections was also assessed, it was concluded that the sheared edge distance is approximately 6 to 7 times bolt hole diameter and that the rolled edge distance effects area insignificant it the conducted study (Sweedan et al., 2013).

This paper attempts to establish the factors that help improve energy absorption capacity of steel to hybrid (steel/GFRP) and steel to GFRP double lap shear connections. The connections had dimensions of 125 mm × 70 mm with various design features such as the use of two and three bolted connections, applying additional GFRP strips, applying adhesive between the steel plate and the internal layer of GFRP and finally the application of adhesive between the clamping plate and the FRP around the bolted area. The specimens were subjected to a 2mm/min monotonic load to complete failure and upon testing, the results were analysed, and relevant results and conclusions were given.

2. Methodology

2.1. Material properties

The control and hybrid specimens were made from 0.8 mm steel plates with a grade of S275 and unidirectional pre-impregnated (prepreg) GFRP. The steel plates were cut by the supplier to the required dimensions of 125 mm ×70 mm to reduce dimensional variations. The dimensions of 125 mm were chosen based on the restrictions imposed by the testing machinery, allowing sufficient part of the sample to be claimed. Dimension of 70 mm corresponds to adopted distance of two bolt holes in the connection with fish plates from previous experiments conducted in Kingston University (Petkune et al., 2014) allowing further comparison of results. Prepreg FRP composites are impregnated with resin during manufacturing for ease of use, advanced finish quality and consistent material behaviour. This specific prepreg GFRP (E722-02 UGE400-02 32%rw) was supplied by TenCate Advanced Composites, UK. FRP Material properties of the unidirectional GFRP used is provided in Table 1 below, derived from conducted tests.

Table 1. Material properties for unidirectional prepreg GFRP.

Material properties for unidirectional prepreg GFRP	
Fibre direction Young's modulus (E_1) GPa	41
Transverse direction Young's modulus (E_2) GPa	10.5
Poisson's ratio ν_{12}	0.312
Poisson's ratio ν_{21}	0.082
Shear modules (G12) GPa	3.3
Shear strength MPa	100
Resin weight (Ignition loss, weight %)	24.21
Ultimate Average Transvers Strength MPa	27

Ultimate Average Tensile Strength MPa	959

The Scotch-Weld™ Epoxy Adhesive DP110 Grey resin used for bonding the samples to the two clamping plates is a high strength two-part resin. The manufacturers data for this resin is indicated in Table 2.

Table 2. Material properties of Scotch-WeldTM Epoxy Adhesive DP110 Grey resin,(3M, n.d.).

Manufacturer Typical Neat Resin Properties	
Density	1.21 g/cm3 (75.5 lbs/ft³) at 23°C (73.4ºF)
Tg (DMTA) after 1 hour @ 120°C (248ºF)	Onset:120°C (248°F); Peak tan δ: 138°C (280ºF)

2.2. Specimens

The specimens were categorised into two main groups; specimens fastened with two bolts and specimens fastened with three bolts, all of which had a width of 70 mm and a length of 125 mm. The bolts used were A4-70 M8 stainless steel bolts with yield strength of 450 MPa. Three samples were tested for each specimen and the average result of the individual specimen was used for the analyses. Varying factors considered were:

- Introducing four additional layers of E722-02 UGE400-02 32%rw (two layers on either side of the specimen), with a fibre orientation of [±45] around the bolted area. These additional layers of FRP increase the thickness of the plate and therefore contribute to a larger area where the bolt bears on the plate. With these additional layers, an increase of connection capacity is intended.
- DP110 Scotch-Weld adhesive was applied around the bolted areas of the connections. The application of adhesive is crucial to reduce slip in the connection and thus aid in developing more stable tension fields in a SSW system.
- An adhesive film layer (EF72) is applied between the steel plate in the hybrid steel/FRP connections and the first layer of GFRP. This adhesive film was applied to reduce the risk of delamination of GFRP layer from steel.
- Pure FRP connections consisting of 8 layers of GFRP were also tested. The 4 additional layers of GFRP layers are for compensating for the removal of the 0.8 mm steel plate in the hybrid steel/FRP connections.

Fibre orientation of $[\pm 45]_{2s}$ was used for connections with eight layers of GFRP. Orientation of fibres for the hybrid steel/FRP connections was$[\pm 45/S/\mp 45]$.
The specimens were placed in a Mayes 100 kN tensile testing machine where they were subjected to a displacement controlled monotonic loading at a rate of 2 mm/min. The adopted testing samples investigates the behaviour of connections close to the middle of the fish plates (mid span of the horizontal and vertical frame boundary elements) in a SSW system that are predominantly in tension. For the part of the infill plate at the corners, the distribution of stresses is more complex as there is a combination of shear and tension. This area needs additional investigation.

For assessment of the energy absorption and mode of destruction, the loading was continued well beyond the point of obtaining the ultimate load capacity of specimens. Figure 1 and Table 2 give information about the geometry, type and number of samples.

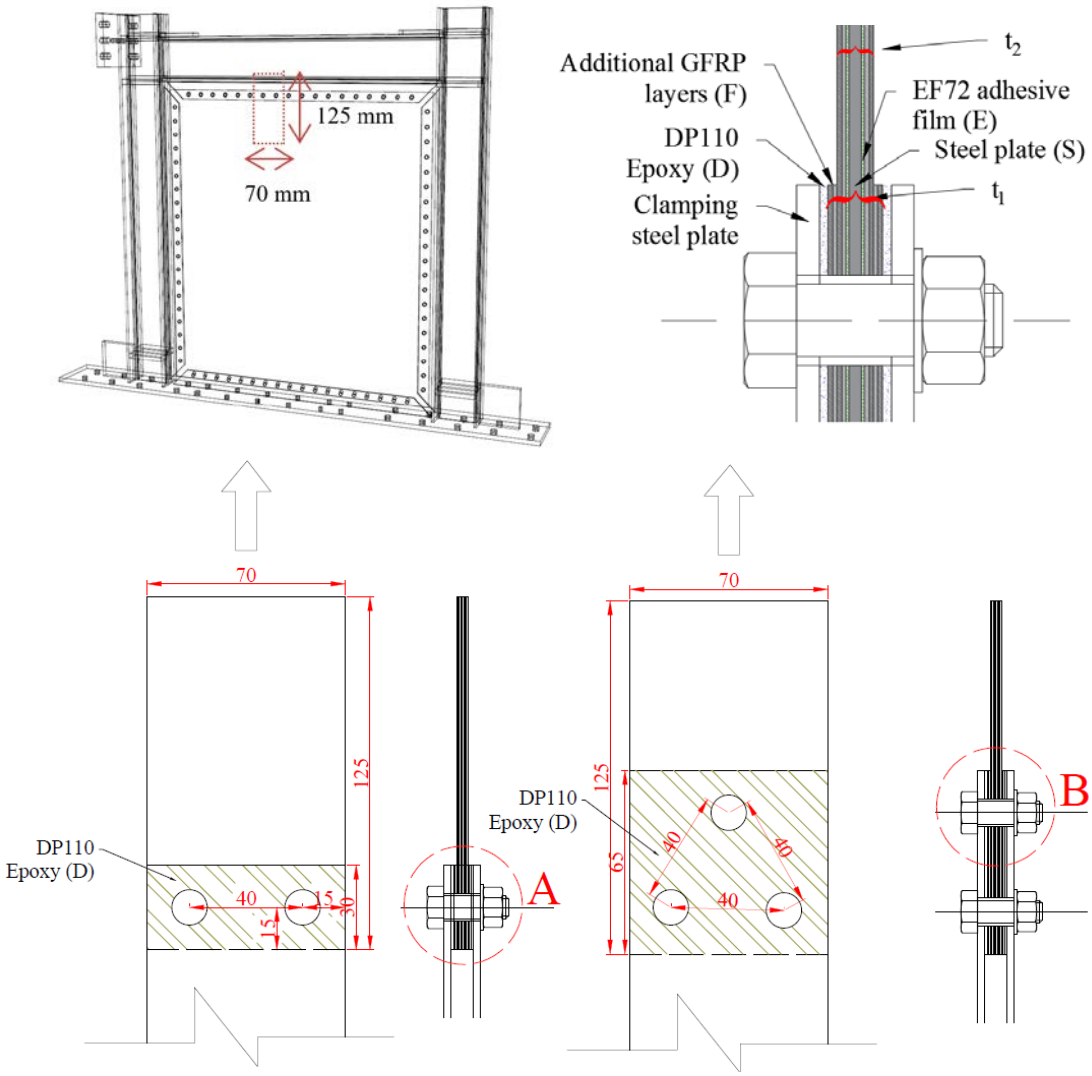

Figure 1. General dimensions of the specimens and cross section; Top Left: Generic SSW system with bolted connection, Top Right: Details of layers for specimens with two and three bolts section A & B, Bottom Left: Two bolted specimen general arrangement, and Bottom Right: Three bolted specimen general arrangement.

As numerous factors involved in these experiments, the following naming system was adopted for all two and three bolted specimens each with individual lettering:

i. C- indicates a control specimen
ii. D- Specimens having DP110 adhesive applied to the bolted area
iii. F- Specimens that incorporate additional two layers of GFRP on either side of the bolted area
iv. FD- Specimens that adopt a combination of additional FRP and adhesive around the bolted area.

Table 3 presents classification of the tested connections where, the two bolted specimens are noted by (A) while the three bolted specimens are noted by (B). The two and three bolted connection groups are divided into three main sub groups. The specimens in the first sub-group (1) are convened based on the fact that the samples consisted of pure unidirectional GFRP material of 8 layers. The second sub-group (2) consists of hybrid steel/GFRP connections with a 0.8 mm steel plate and 4 layers of GFRP. The third sub-group (3) has the exact same type of samples as subgroup 2, with the exception that all the connections in the specimens in the subgroup have a layer of EF72 adhesive film applied between the steel plate and first internal layer of GFRP.

Table 3. Specimen specifications.

Group	Specimen	No. of Bolts	Steel plate (S)	GFRP (G)	No. of layers of GFRP	Additional 4 layers of GRP area (F)	EF72 adhesive film (E)	DP110 Epoxy (D)	Thickness t1(mm)	Thickness t2(mm)
A1	**C** (2G8)	2		✓	8				2.13	2.13
	D (2G8D)	2		✓	8			✓	2.13	2.13
	F (2G8F)	2		✓	8	✓			3	2.2
	FD (2G8FD)	2		✓	8	✓		✓	3	3
A2	**C** (2SG4)	2	✓	✓	4				1.82	1.82
	D (2SG4D)	2	✓	✓	4			✓	1.92	1.92
	F (2SG4F)	2	✓	✓	4	✓			3.05	2
	FD (2SG4FD)	2	✓	✓	4	✓		✓	3.05	2
A3	**C** (2SG4E)	2	✓	✓	4		✓		2.08	2.08
	D (2SG4ED)	2	✓	✓	4		✓	✓	2.08	2.08
	F (2SG4FE)	2	✓	✓	4	✓	✓		3.15	2.1
	FD (2SG4FED)	2	✓	✓	4	✓	✓	✓	3.15	2.1
B1	**C** (3G8)	3		✓	8				2.2	2.2
	D (3G8D)	3		✓	8			✓	2.2	2.2
	F (3G8F)	3		✓	8	✓			3.06	2.07
	FD (3G8FD)	3		✓	8	✓		✓	3.06	2.07
B2	**C** (3SG4)	3	✓	✓	4				2	2
	D (3SG4D)	3	✓	✓	4			✓	2	2
	F (3SG4F)	3	✓	✓	4	✓			2.93	1.9
	FD (3SG4FD0	3	✓	✓	4	✓		✓	2.93	1.9
B3	**C** (3SG4E)	3	✓	✓	4		✓		2.1	2.1
	D(3SG4ED)	3	✓	✓	4		✓	✓	2.1	2.1
	F (3SG4FE)	3	✓	✓	4	✓	✓		3.09	2.09
	FD (3SG4FED)	3	✓	✓	4	✓	✓	✓	3.09	2.09

2.3. Specimens preparation

Prior to the application of the EF72 adhesive film, the steel plate surface was abraded using sandpaper and cleaned using acetone to remove any rust and/or oils that could compromise the bonding between the first layer of GFRP and the steel plate. Curing of the samples was done

by the vacuum bag method at 120 °C. The specimens were placed between two thick steel plates and wrapped in breathing fabric, before placing it inside a sealed bag, and connected to a 1 bar vacuum pump. The curing procedure was followed according to the manufacturer's specification, where the specimen was kept at 120 °C for one hour. Figure 2 illustrates the steps taken to prepare the specimens.

After the curing, the specimen's edges were sanded down and cleaned to give the exact

specified dimensions, and 9.5 mm diameter holes were drilled to accommodate for the bolts.

Figure 3 shows the final specimens after curing and sanding ready for the test.

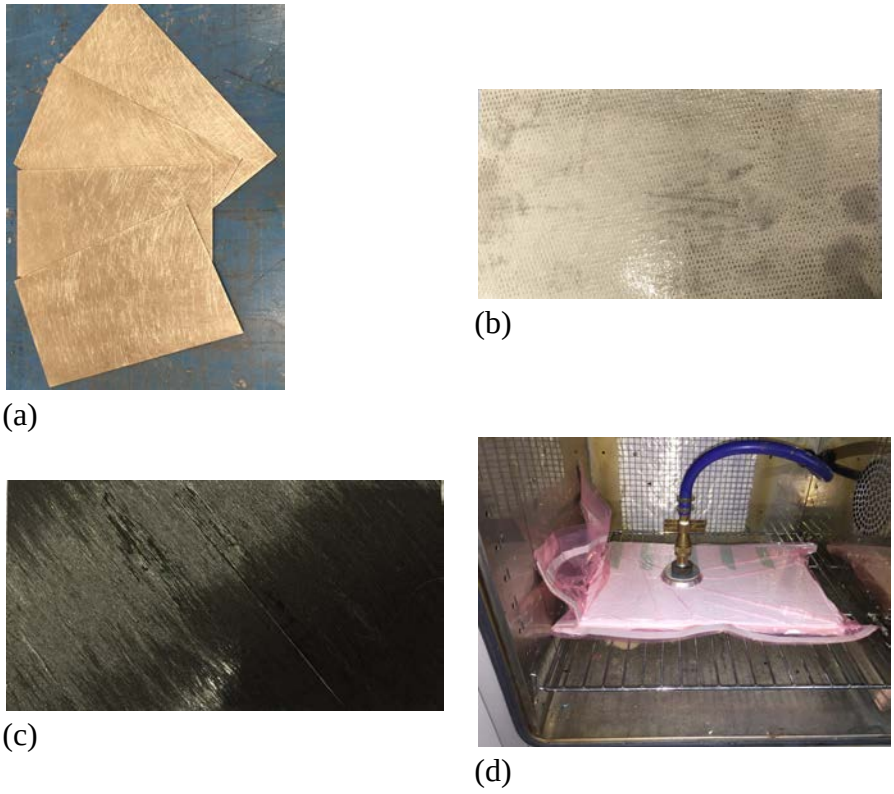

Figure 2. Specimen preparation: (a) Abraded steel plates, (b) application of EF72 adhesive film, (c) placement of GFRP prepreg at ±45 orientations, and (d) curing using oven in a sealed vacuumed bag.

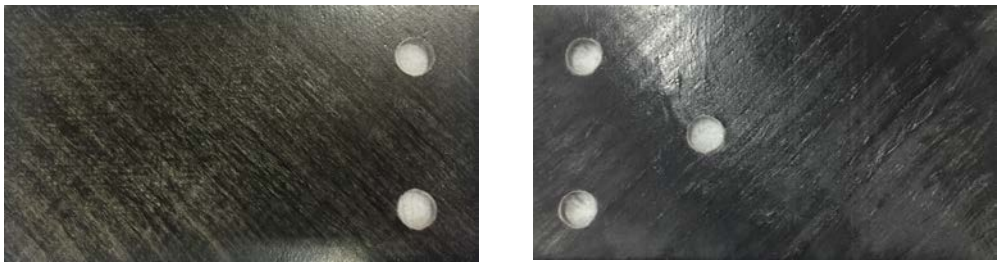

Figure 3. Specimens after curing, drilling holes and sanding down.

Post fabrication and prior to installation of specimens in the loading rig, the specimens were abraded around the bolted area and clamped between two steel plates. For the specimens bonded with DP110 adhesive, the bonding area was also slightly abraded to increase the surface area and cleaned with acetone. A thin layer of DP110 was applied and the two plates were placed and clamped at the same torque of 18 N.m.

3. Results and Analysis

Energy absorption and load capacity were the two main factors that were studied. The enclosed area under the load displacement graphs allows for the estimation of the absorbed energy by the specimens. Due to the numerous amounts of specimens tested and in order to determine the level of contribution of each configuration to both energy absorption and load capacity, the results and analysis are divided into groups as described below.

3.1. Two bolted connections (Group A)

The two bolted connections are divided into three main sub groups:
The specimens in the first sub-group (Group A1) are convened based on the samples consisted of pure unidirectional GFRP material of 8 layers. The control sample for this group is a specimen with 2 bolts and 8 layers of GFRP (2G8). The varying factors in this group are the application of adhesive DP110 around the bolted area (D) or the application of additional GFRP strips around the bolted area (F) as well as the simultaneous application of both factors (FD).
The second sub-group (Group A2) consists of hybrid steel/GFRP connections with a 0.8 mm steel plate and 4 layers of GFRP. The specimen 2SG4 is chosen as a control specimen. The varying factors are similar to those of the pure GFRP samples in group A1 (D, F and FD).
The third sub-group (Group A3) has the exact same type of samples as the group A2. However, with the exception that all the connections in the third group have a layer of EF72 adhesive film applied between the 0.8 mm steel plate and first internal layer of GFRP. The control specimen is 2SG4E and the subsequent specimens in the group are D, F, and FD. For comparison, complete failure of the sample is defined as the point where the applied load is reduced to more than 2 kN.
Load-displacement behaviours for the pure GFRP samples in group A1 are shown in Figure 4. The specimen (D), with the applied DP110 around the bolted area of the connection exhibited an increase in ultimate load capacity of 104% relative to the control specimen. A high increase in ultimate load capacity of 90% could also be seen in sample (F). Although 2G8D showed a higher increase in load capacity, the maximum displacement the specimen reached before complete failure was 16 mm resulting in a 107 % increase in energy absorption. The sample with the additional layer of GFRP (F) exhibited a 122% increase in energy absorption.
Application of both additional layers of GFRP and DP110 adhesive around the bolted area (FD) will result in an even higher increase in energy absorption and ultimate load carrying capacity as shown in Table 4

Table 4. Variations in ultimate load capacity and energy absorption in comparison to the control specimen in group A1.

Group A1	Variation in ultimate load capacity compared to control	Variation in energy absorption compared to control
2G8 (Control)	–	–
F	90%	122%
D	104%	107%
FD	151%	164%

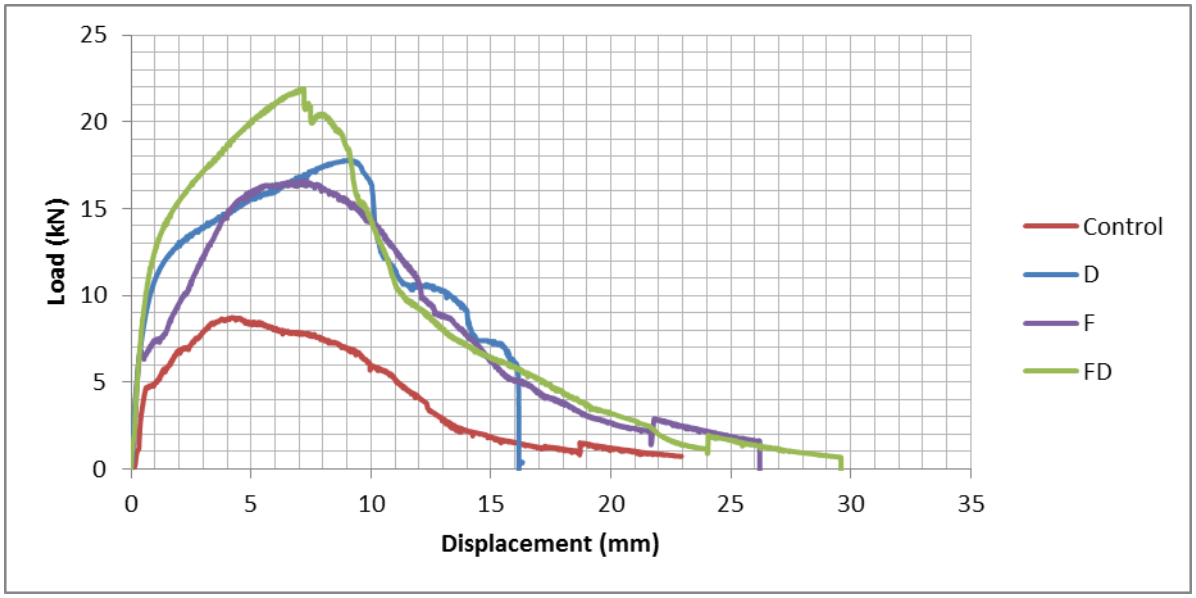

Figure 4. Load-displacement of connections made from GFRP with 2 bolts (Group A1).

Figure 5 illustrates the load-displacement curve for samples in group A2. These hybrid steel/GFRP samples consist of 0.8 mm steel plate replacing 4 of the 8 layers of GFRP in the pure GFRP connections. The variation of factors are like those of the pure GFRP connections and the control sample is 2SG4. When comparing the connections with additional GFRP around the bolted area (F) and the connections with additional adhesive around the same area (D), the latter exhibited higher initial load capacity due to reduction of slip between the clamping plates. Specimens in (D) exhibited an increase in ultimate load capacity and energy absorption of 92% and 105%, respectively. The variations in energy absorption and ultimate load capacity relative to the control specimen are shown in Table 5.The results in Table 5 are less pronounced than in Table 4 due to the higher capacity of the control sample for the hybrid specimens.

Table 5. Variations in ultimate load capacity and energy absorption in comparison to the control specimen in group A2.

Group A2	Variation in energy dissipation compared to control	Variation in energy dissipation compared to control
2SG4 (Control)	-	-
F	30%	29%
D	53%	54%
FD	92%	105%

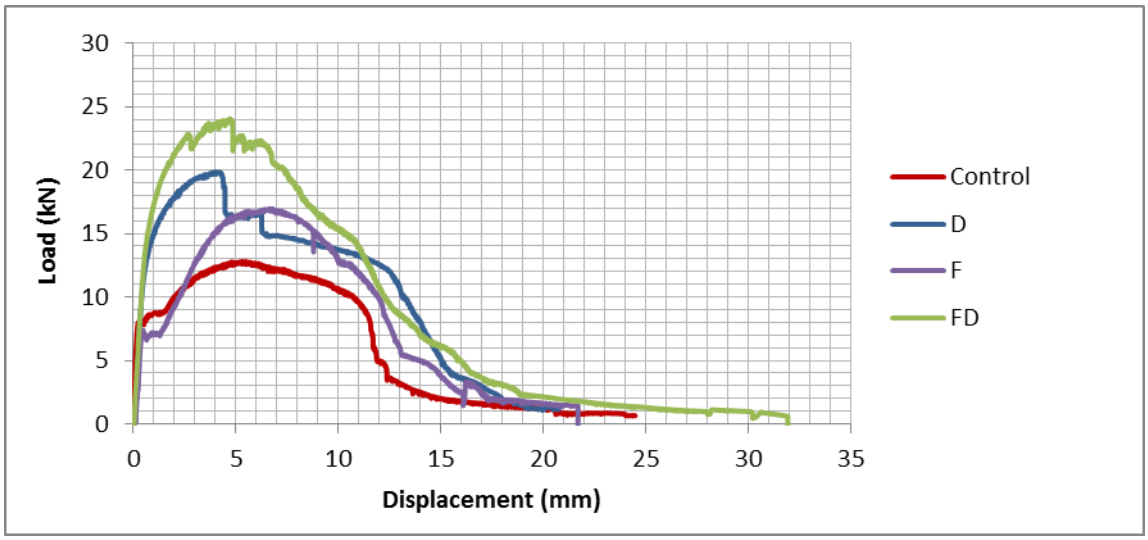

Figure 5. Load-displacement of hybrid connections with 2 bolts, without EF72 adhesive film (Group A2).

Finally, sub-group A3 consists of all the specimens that have an adhesive film between the first internal layer of GFRP and the 0.8mm steel plate to reduce the risk of delamination. The group consists of 4 types of specimens with the same varying factors as group A2 and the control in this group is 2SG4E. Figure 6 shows load-displacement behaviour for all specimens. The highest ultimate load capacity and energy absorption is achieved by (FD), with an increase of 107% and 127%, respectively. It is clear from the graph that using both additional layers of GFRP and adhesive around the bolted area increases the connection's ultimate load capacity and energy absorption even further than if they were to be used individually. The observed sudden drop in load for D and & FD specimens is due to the partial slip of the sample between the clamping plates as a result of the additional adhesive around the bolted area. The variations in load capacity and energy absorption compared to control specimen are summarised in Table 6.

Table 6. Variations in ultimate load capacity and energy absorption in comparison to the control specimen in group A3.

Group A3	Variation in ultimate load capacity compared to control	Variation in energy dissipation compared to control
2SG4E (Control)	-	-
F	32%	44%
D	56%	72%
FD	107%	127%

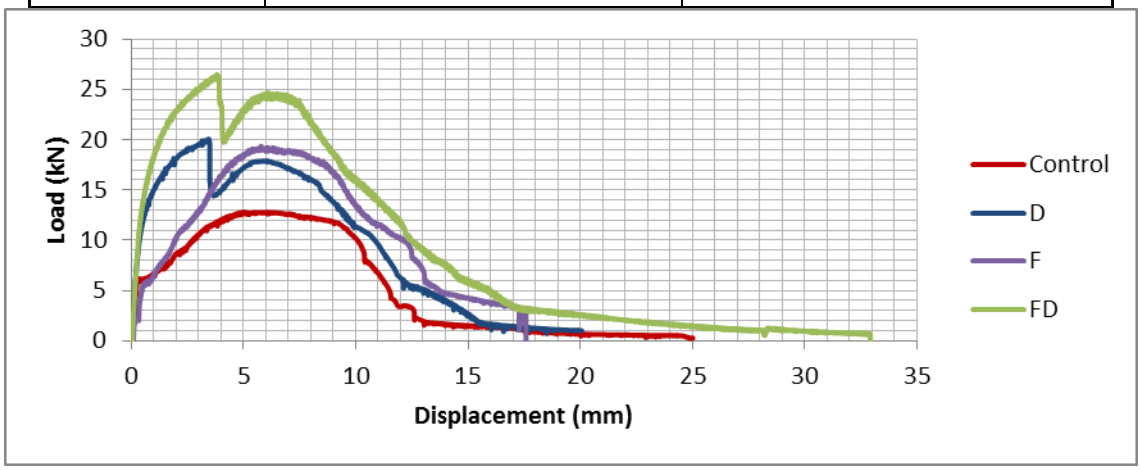

Figure 6. Load-displacement for specimens with 2 bolts, with adhesive film between the steel plate and the initial GFRP layer (Group A3).

The bar chart in Figure 7 compares the ultimate load carrying capacity and energy absorption achieved by the two bolts specimens in the three groups. The application of DP110 adhesive increases the ultimate load capacity for all the specimens and contributes to a higher initial stiffness due to reduced slippage between the clamping plates and the connection. Application of additional layers of GFRP increased the ultimate load capacity and energy absorption, but in most cases this increase was less significant than the application of DP110 adhesive as shown in Tables 4, 5 and 6. By comparing sample (FD) in group B and (FD) in group C, it is clear that the application of a film adhesive layer between the initial internal layer of GFRP and the 0.8 mm steel plate does not result in any noticeable increase in the load capacity and energy dissipation. However, when looking at a hybrid shear wall system the application of the adhesive film affects the overall behaviour of the system. Petkune et al. [17] stated that the application of adhesive film in a hybrid steel/CFRP shear wall system significantly improves the behaviour of the shear wall due to postponement of delamination of the CFRP layers from steel plate in the hybrid steel/CFRP infill plate.

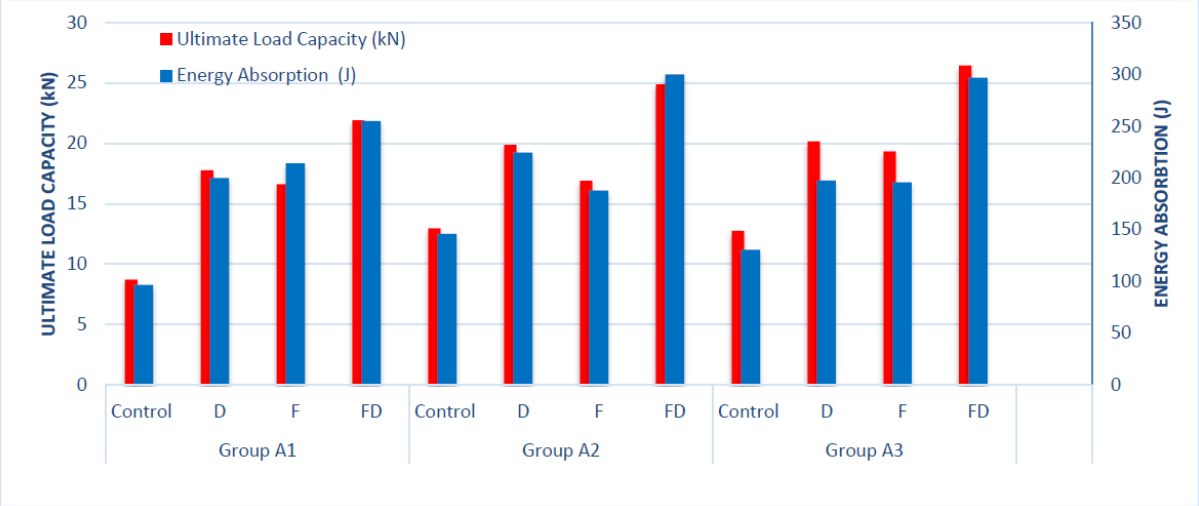

Figure 7. Energy absorption and maximum load capacity for specimens with two bolts.

3.2. Modes of Failure for Two Bolted Connections

Common modes of failure observed in the tested connections are bearing, shear (Figure 8 ii) and cleavage (Figure 8 iii), where the former is a combination of both tensions and shear failure. The images in Figure 8 show the different modes observed in some of the specimens where specimen F in group A1 displayed shear out of the FRP and the hybrid specimen FD in group A2 exhibited cleavage type failure. It is observed that for the FRP only specimens, when adhesive is applied around the bolted area, the failure is outside the bolted zone as can be seen in Figure 8 (v).

For the other samples the variety of different failure modes are observed for each of the groups. Lack of direct correspondence between the types of samples and their failure mode is due to simultaneous influence of a wide range of factors, such as stress distribution in multi-layered strata with complicated application of the load.

Figure 8. Modes of failure in two bolt specimens. Starting from the left: (i) sample before testing, (ii) shear, (iii) cleavage, (iv) combination of both shear out and cleavage and (v) failure at mid-section of plate.

3.3. Three bolted connections (Group B)

The three bolted specimens are grouped in a similar way to the two bolted specimens.

1- Group B1 is made from 8 layers of unidirectional GFRP only consisting of Control (3G8), D (3G8D), F (3G8F) and FD (3G8FD) specimens.

2- Group B2 are hybrid steel/GFRP specimens with 2 layers of GFRP on either side of a 0.8mm steel plate consisting of Control (3SG4), F (3SG4F), D (3SG4D), and FD (3SG4FD) specimens.

3- Group B3 are hybrid specimens, with the application of an adhesive film between the steel plate and the first internal GFRP layer to reduce the risk of delamination, consisting of Control (3SG4E), D (3SG4ED), F (3SG4FE) and FD (3SG4FED) specimens.

The varying factors within group B1 are the application of additional layers of GFRP and/or the application of DP110 adhesive around the bolted area. Those factors are investigated separately and when simultaneously combined. The control specimen in this group was 3G8 which is the specimen with 8 layers of GFRP only. The load-displacement behaviour for this group is shown in Figure 9.
Figure 9 shows that the specimen with 8 layers of GFRP and DP110 adhesive around the bolted area of the connection (D) exhibited approximately 44% increase in the load carrying capacity whereas the energy absorption was reduced by approximately 36% in comparison with the control specimen. The reason behind the decrease in energy absorption can be merited to the high increase in load capacity and the stiffness of the connection resulting in a more sudden and abrupt failure of the GFRP material, as can be seen with the steep decline in the load-displacement curve. Specimen F shows a lower increase in load capacity compared to specimen D as can be seen in Table 7. However, this specimen does not show any reduction in energy dissipation.

Table 7. Variation in ultimate load capacity and energy absorption in comparison with the control specimen in group B1.

Group B1	Variation in ultimate load capacity compared to control	Variation in energy absorption compared to control
3G8 (Control)	–	–
F	16%	1%
D	44%	-36%
FD	5%	-35%

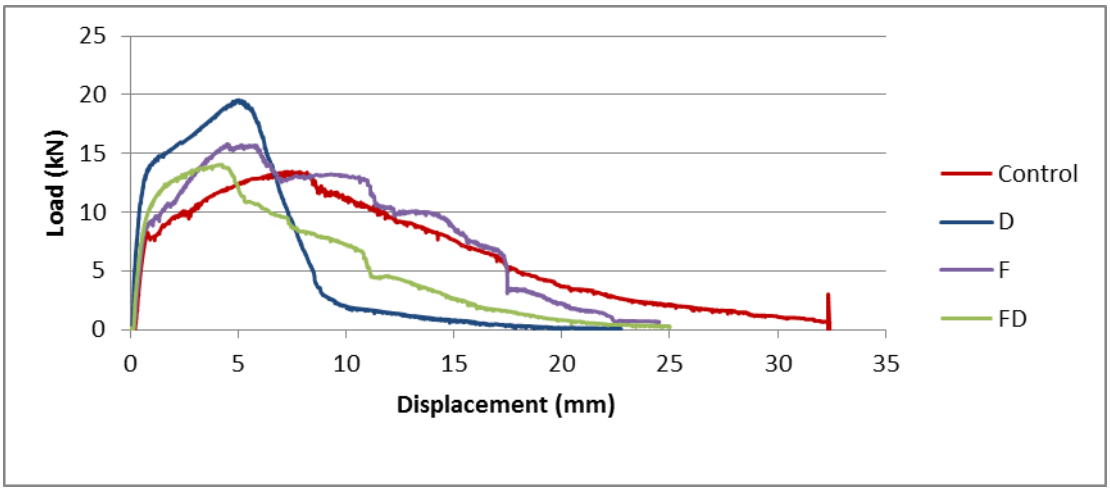

Figure 9. Load-displacement of pure GFRP connections with 3 bolts for group B1.

Load-displacement graph for Group B2 is shown in Figure 10. The group consists of specimens with hybrid steel/GFRP material where the central 0.8 mm internal plate is laminated with 2 layers of GFRP on either side. Group B2 have the same varying factors as that of the previous group B1. The control specimen in this group is 3SG4. An increase in ultimate load capacity and energy absorption of 8% and 11% respectively is noticed when specimen D is compared to the control specimen. However, specimen F proves to have a higher increase in ultimate load capacity and energy absorption, reaching 14% and 64% respectively as shown in Table 8. The application of both adhesive and additional GFRP strips around the bolted area results in a slight increase in ultimate load capacity of 8% and a 46% increase in energy absorption relative to the control specimen.

Table 8. Variations in ultimate load capacity and energy absorption in comparison with the control specimen in group B2.

Group B2	Variation in ultimate load capacity compared to control	Variation in energy absorption compared to control
3SG4 (Control)	-	-
F	14%	64%
D	8%	11%
FD	8%	46%

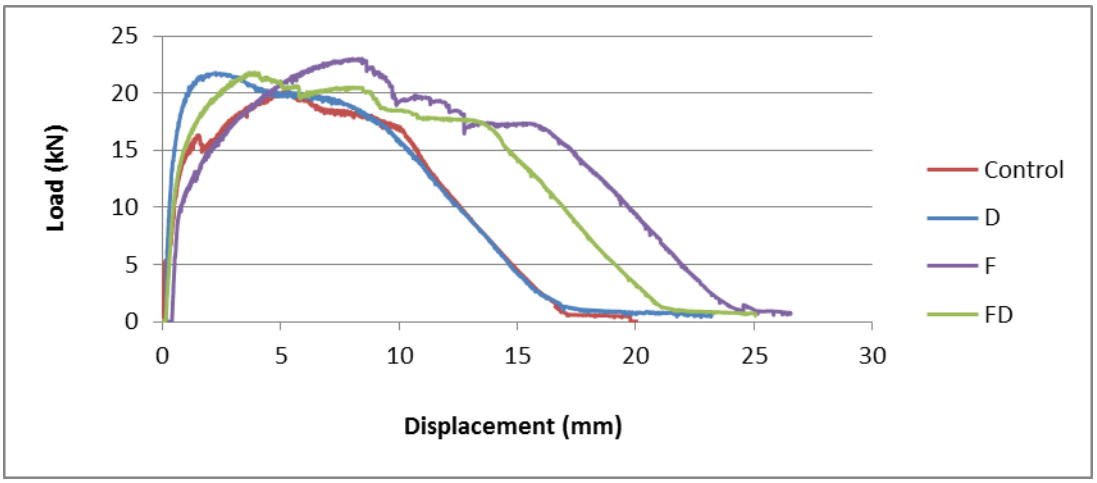

Figure 10. Load-displacement of hybrid connections with 3 bolts, without EF72 adhesive film for group B2.

Group B3 encapsulates the hybrid steel/GFRP specimens that incorporate an adhesive film layer between the steel plate and the initial GFRP layer as a measure to reduce the risk of delamination. The load- displacement behaviour of the specimens in this group is shown in Figure 11. The variations within the group include the control specimen, D, F and FD.

3SG4E is the control specimen for this group. Table 8 summarises variation in ultimate load capacity and energy absorption for specimens F, D and FD in group B3 as percentages change relative to the control specimen. The data shows that D displayed minimal increase of 4% and 1% in both ultimate load capacity and energy absorption, respectively. The application of additional layers of GFRP around the bolted area in specimen F increases the bearing area for the bolts and eventually increases the load capacity and energy dissipation. Table 9 shows that specimen F exhibited a 22% increase in ultimate load capacity and 83% increase in energy absorption relative to control sample.

Table 9. Variations in ultimate load capacity and energy absorption in comparison with the control specimen in group B3.

Group B3	Variation in ultimate load capacity compared to control	Variation in energy dissipation compared to control
3SG4E (Control)	-	-
F	22%	83%
D	4%	1%
FD	22%	54%

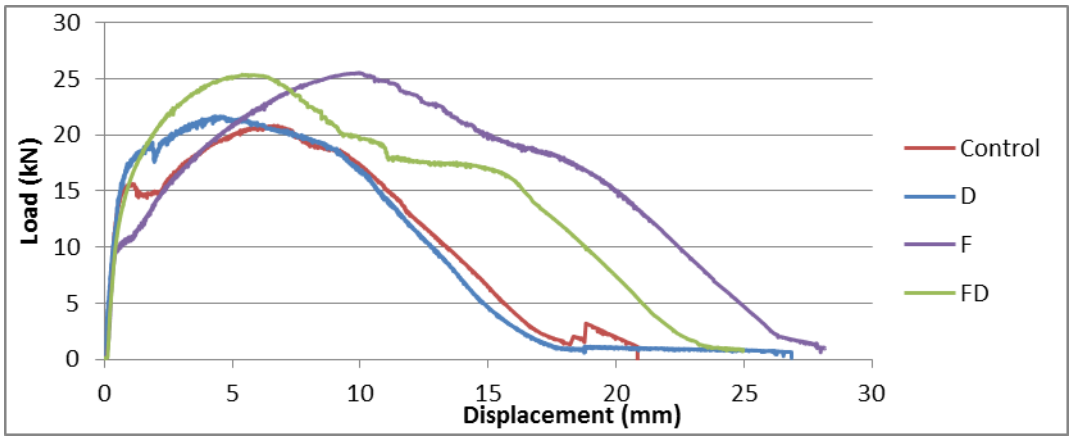

Figure 11. Load-displacement for specimens with 3 bolts, with an adhesive film between the steel plate and the first GFRP layer in Group B3.

Similar ultimate load capacity and slightly lower energy absorption are observed for specimen FD when comparing it to specimen F. This can be attributed to the application of adhesive around the bolted area resulting in a stiffer connection and eventually failure in the plate end of the specimen (thinner part). It can be seen from the load-displacement in Figure 11 that specimen F displayed lower stiffness but resulted in slightly higher energy absorption, while specimen FD performed the opposite behaviour.

Figure 12 was produced to give an indication of how each varying factor in this experiment influences the behaviour of all three bolted connections in aspects of energy absorption and ultimate load capacity. Looking at the bar chart, it is evident that the application of additional layers around the bolted area (type F) increases the load capacity and energy dissipation of the specimen. However, the application of DP110 (type D) will have minimal effect on most of the specimens because of the stiff bond achieved between the clamping plate and the specimen, resulting in a mixed failure mode located in the thinner part of the connection (t_2 in Figure 1). Due to the failure of the plate part of the connection in specimen's D and F in group B1, these two types of specimens presented a lower load capacity and energy absorption than expected. The specimens that failed partially or predominantly outside the bolted area shaded as in Figure 12. The obtained values illustrated in Figure 12 are the real values, however they could be exceeded if the part of the sample outside the connection area is stronger, so the failure is achieved in the bolted area of the connection.

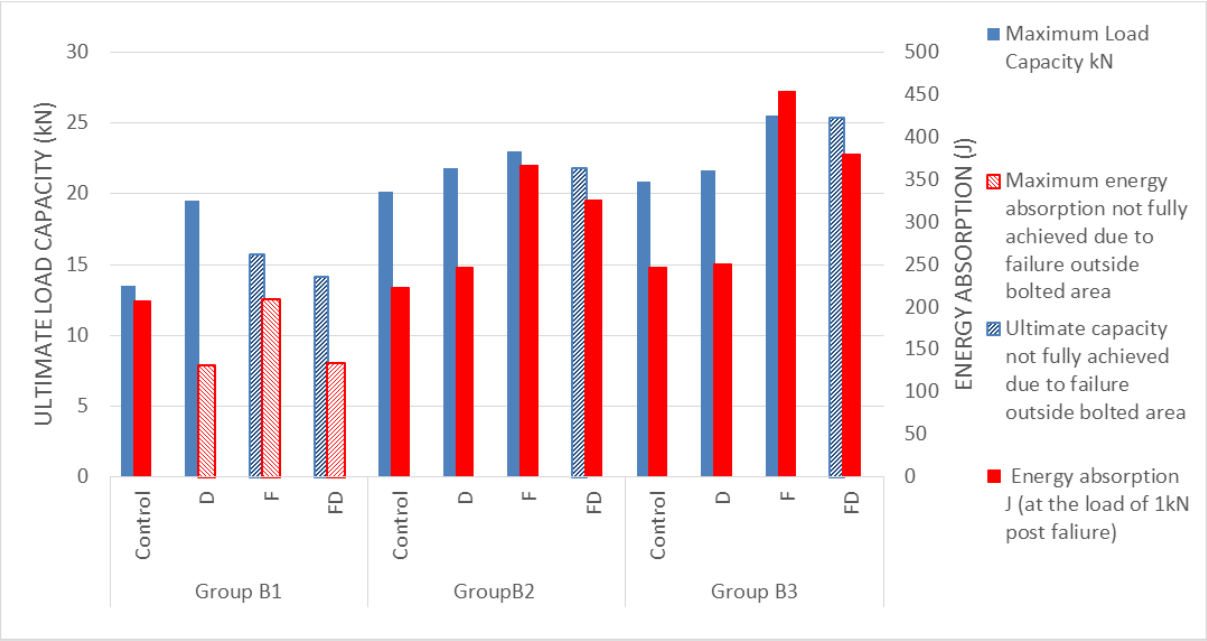

Figure 12. Energy absorption and maximum load capacity for specimens with three bolts.

3.4. Modes of Failure for Three Bolted Connections

Few of the specimens with three bolts exhibited a mixed mode of failure, where the specimen failed at the first row of bolts as well as the thinner part of the plate indicating the connection is stronger than the plate segment of the specimen. In some cases, the specimens failed completely outside the connection resulting in a lower energy absorption and ultimate load capacity than expected.

The images in Figure 13 represent modes of failure in some of the tested specimens. The control in group B3 demonstrated tearing failure of the internal steel plate at the first row of bolts with the GFRP tearing diagonally running through the first row, this was also observed in specimen D in group B3. Specimen F in group B1 exhibited fibre failure in the area outside the bolted area of the specimen.

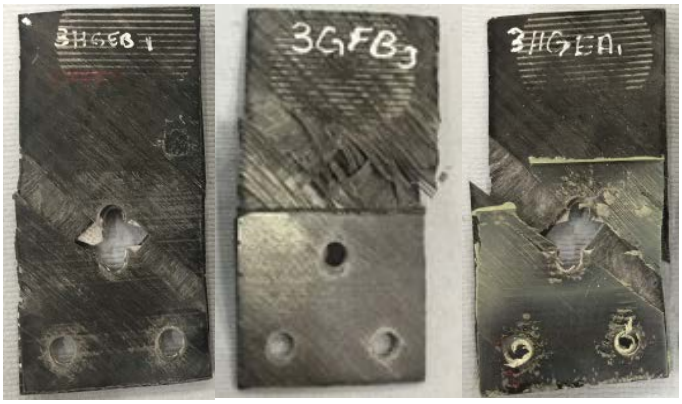

Figure 13. Failure modes in three bolted specimens: (left) Control in Group B3, (middle) F in Group B1 & (right) D in Group B3.

3.5. Comparison between two and three bolted connections

Figure 14 compares the performance of the plates connected by two bolts (representing a single row of bolts in a SSW system) and the ones by three bolts (representing two rows of bolts in a SSW system). In most cases the three bolted connections had a higher load capacity than that of their equivalent specimens with two bolts. The highest difference in load capacity was achieved between the control in group A1 and the control in group B1 reaching an increase of 58% for the later specimen. This can be attributed mainly to the mode of failure where specimen D in group B3 exhibited failure in the plate part of the sample (t_2) in Figure 1 which will result in a lower ultimate load capacity than estimated. The ultimate load capacity of specimens that exhibited this mode of destruction have been shaded indicating that they have a potential for a higher ultimate capacity as can be seen in Figure 14. Moreover, the application of additional GFRP and/or adhesive will reduce the difference in load capacity between the two and three bolted specimens. This indicates that the application of these factors is more effective in the two bolted specimens. The main reason for the increase in the load capacity between the control in group A1 and the control in group B1 is due to the higher contribution of bearing capacity of the bolts for the specimens that have no adhesive. As slip occurs the bolts start bearing the specimens, giving the specimens with a higher number of bolts a higher load capacity.

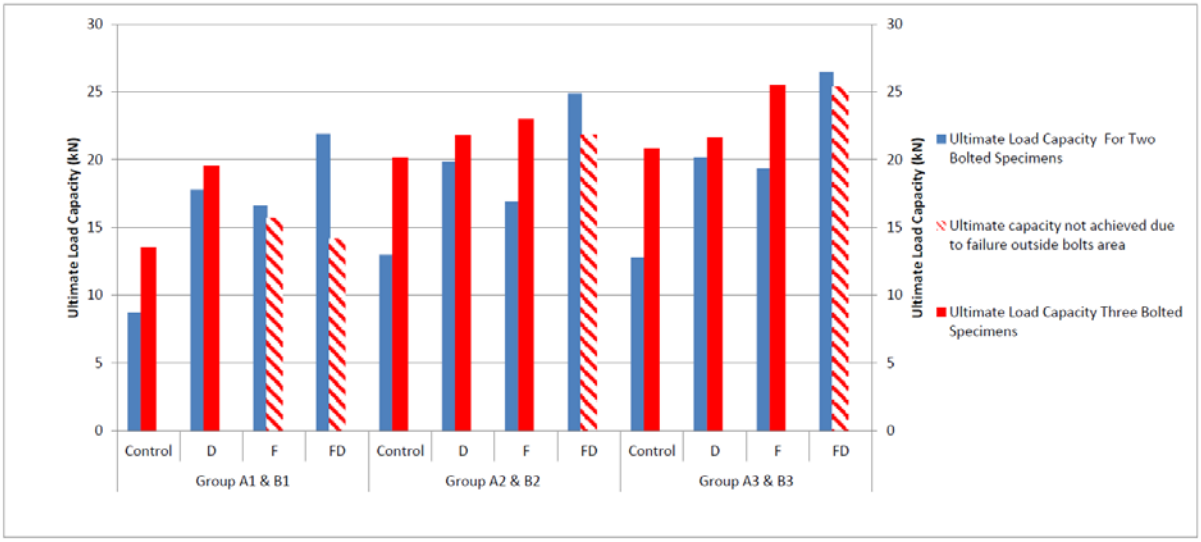

Figure 14. Comparing load capacity of specimens with two and three bolts connections.

The energy absorption of all specimens is shown in Figure 15. As for the load capacity, most of the three bolted specimens exhibited higher energy absorption than the two bolted specimens with the same design. The three bolted specimens that did not present a higher increase in energy absorption than the two bolted specimens were those which failed outside the joint area. The highest increase in the energy absorption is achieved by specimen F in group B3.

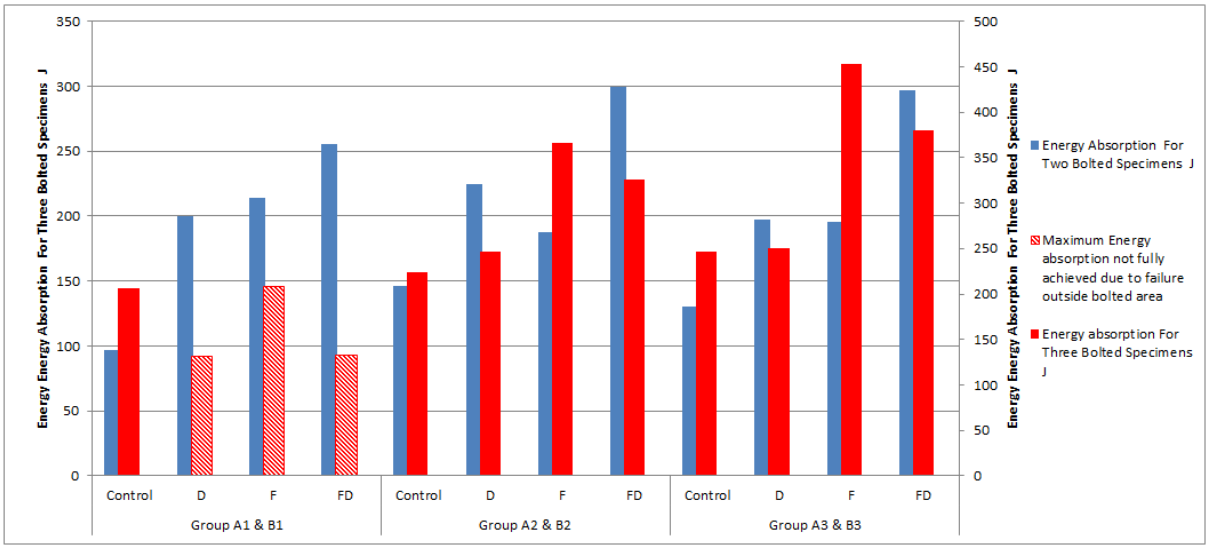

Figure 15. Comparison of energy absorption of specimens with two and three bolts connections.

4. Conclusion

Designing proper connection between infill plate and surrounding fish plate in hybrid steel/FRP and pure FRP shear wall systems was the aim of this study. The objective was to design a connection with maximum energy absorption and highest ultimate load carrying capacity.
The two design variants that have been considered were two and three bolted connections. In each variant different design details such as bonding, adding film adhesive between the steel and GFRP laminate and using extra GFRP strip over the bolts were considered. Various specimens containing each of these features were made and monotonically tested in a tensile testing machine. By analysing and comparing results from both, the two and three bolted specimens, the following conclusions can be made:

1- Application of adhesive around the bolted area results in a higher increase in ultimate load capacity and energy absorption for 2 bolted specimens in comparison with 3 bottled specimens.
2- Additional layers of GFRP around the bolted area of the specimens have a beneficial effect for both two bolted and three bolted specimens, increasing both ultimate load capacity and energy absorption. However, the increase in ultimate load capacity is more prominent in the two bolted specimens.
3- Additional epoxy layer (E) between the steel plate and the adjacent GFRP layers at the zone of bolting does not contribute significantly to the increase in the capacity and energy absorption.
4- There is an increase in ultimate load capacity when applying adhesive between the sample and the clamping plates (representing the fish plate connection), for the three-bolted pure GFRP specimens (Group B1). This increase is accompanied with a reduction in energy absorption Table 5.
5- Specimens F & FD in group (B1) had a reduced ultimate load capacity and energy absorption due to the mode of failure observed. For them, the plate part of the specimen failed before the connection could reach its full capacity.

This study indicates the effective approaches to increase the ultimate load carrying capacity and energy absorption for connections in hybrid and pure FRP shear wall systems.

Reference

3M, n.d. 3M™ Scotch-Weld™ Epoxy Adhesive DP110 Gray | 3M United States [WWW Document]. URL https://www.3m.com/3M/en_US/company-us/all-3m-products/~/3M-Scotch-Weld-Epoxy-Adhesive-DP110-Gray/?N=5002385+3293242433&rt=rud (accessed 9.1.18).

Abou El-Hamd, O.R., Sweedan, A.M.I., El-Sawy, K.M., 2018. Experimental and numerical study of the parameters controlling the behavior of double-lap connections of steel plates bolted to hybrid FRP strips. Thin-Walled Struct. 125, 140–151. https://doi.org/10.1016/J.TWS.2018.01.018

American Institute of Steel Construction, 2016. ANSI/AISC 341-16, Seismic Provisions for Structural Steel Buildings, Seismic Provisions for Structural Steel Buildings. https://doi.org/111

Architecture & Building Press, 1998. Technical Specification for Steel structure of Tall Buildings, JGJ 99 – 98. Beijing, China.

Bahrebar, M., Kabir, M.Z., Hajsadeghi, M., Zirakian, T., Lim, J.B.P., 2016. Structural performance of steel plate shear walls with trapezoidal corrugations and centrally-placed square perforations. Int. J. Steel Struct. 16, 845–855. https://doi.org/10.1007/s13296-015-0116-y

Bhowmick, A., Grondin, G., Driver, R., 2014. Nonlinear seismic analysis of perforated steel plate shear walls. J. Constr. Steel Res. 94, 103–113. https://doi.org/10.1016/j.jcsr.2013.11.006

Choi, I., Park, H., 2008. Cyclic test for framed steel plate walls with various infill plate details, in: The 14 Th World Conference on Earthquake Engineering . Beijing, China .

Dakhel, M., Donchev, T., Hadavinia, H., Limbachiya, M., Engineering, A., 2016. Energy Dissipation Characteristics Of Connections For Hybrid And FRP Infill Plates For Shear Walls, in: The 8th International Conference on Fibre-Reinforced Polymer Composites in Civil Engineering (CICE). Hong Kong.

Gardner, A., 2015. Stability of buildings Part 3 : March 2015. The Institution of Structural Engineers.

Hai, N.D., Mutsuyoshi, H., 2012. Structural behavior of double-lap joints of steel splice plates bolted / bonded to pultruded hybrid CFRP / GFRP laminates. Constr. Build. Mater. 30, 347–359. https://doi.org/10.1016/j.conbuildmat.2011.12.001

Ilg, P., Hoehne, C., Guenther, E., 2016. High-performance materials in infrastructure: a review of applied life cycle costing and its drivers e the case of fiber-reinforced composites. J. Clean. Prod. 112, 926–945. https://doi.org/10.1016/j.jclepro.2015.07.051

Japan. Kensetsushåo. Jåutakukyoku. Kenchiku Shidåoka., Nihon Kenchiku Sentåa., 2004. The Building standard law of Japan. Building Center of Japan.

Manalo, A.C., Mutsuyoshi, H., Asamoto, S., Aravinthan, T., Matsui, T., 2008. Mechanical behavior of hybrid FRP composites with bolted joints, in: 20th Australasian Conference on the Mechanics of Structures and Materials (ACMSM 20): Futures in Mechanics of Structures and Materials. Toowoomba, Australia.

Nateghi-Alahi, F., Khazaei-Poul, M., 2012. Experimental study of steel plate shear walls with infill plates strengthened by GFRP laminates. J. Constr. Steel Res. 78, 159–172. https://doi.org/10.1016/j.jcsr.2012.07.002

Petkune, N., Donchev, T., Hadavinia, H., Limbachiya, M., 2014. Investigation in connections between steel, composite and hybrid structural elements, in: MCM-2014: Mechanics of Composite Materials. Riga, Latvia.

Rosner, C., Rizkalla, S.H., 1995. Bolted connections for fiber-reinforced composite structural members: analytical model and design recommendations. J. Mater. Civ. Eng. 232–238.

Sabelli, R., Bruneau, M., 2006. Design Guide 20: Steel Plate Shear Walls.

Sarkisian, M., Wang, D., Lee, S., John, N., 2011. World's Tallest Steel Shear Walled Building. Counc. Tall Build. Urban Habitat CTBUH.

Seilie, I., Hooper, J., 2005. Steel Plate Shear Walls: Practical Design and Construction, in: North American Steel Construction Conference .

Shekastehband, B., Azaraxsh, A., Showkati, H., 2017. Experimental and numerical study on seismic behavior of LYS and HYS steel plate shear walls connected to frame beams only. Arch. Civ. Mech. Eng. 17, 154–168. https://doi.org/10.1016/J.ACME.2016.09.006

Sweedan, A.M.I., El-Sawy, K.M., Alhadid, M.M.A., 2013. Interfacial behavior of mechanically anchored FRP laminates for strengthening steel beams. J. Constr. Steel Res. 80, 332–345. https://doi.org/10.1016/j.jcsr.2012.09.022

Tsai, K., Li, C., Lin, C., Tsai, C., 2010. Cyclic tests of four two-story narrow steel plate shear walls — Part 1 : Analytical studies and specimen design 775–799. https://doi.org/10.1002/eqe

Turvey, G.J., 2000. Bolted connections in PFRP structures 146–156.

Yadollahi, Y., Pakar, I., Bayat, M., 2015. Evaluation and comparison of behavior of corrugated steel plate shear walls. Lat. Am. J. Solids Struct. 12, 763–786.

Zhou, A., Zhao, L., 2013. Connection Design for FRP Structural Members, in: Zoghi, M. (Ed.), The International Handbook of FRP Composites in Civil Engineering. CRC Press, pp. 171–190.